Results in Engineering 25 (2025) 104101

Contents lists available at ScienceDirect

Results in Engineering

journal homepage: www.sciencedirect.com/journal/results-in-engineering

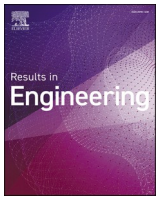

Research paper

Shear strength and behavior of eco-friendly RC corbels

Kadhim Z. Naser *, Abdulamir Atalla Almayah, Abdulnasser M. Abbas

Department of Civil Engineering, College of Engineering, University of Basrah, Basrah 61004, Iraq

ARTICLE INFO

Keywords:
Corbel
Recycled aggregate
Energy absorption
Shear capacity
Initial stiffness
Cracking pattern
Shear span- effective depth ratio

ABSTRACT

The use of efficient and environmentally friendly materials is a priority in the construction industry. In this study, the behavior of reinforced concrete corbels made of recycled concrete aggregate (RCA) was investigated. Twenty models were created and categorized into five Groups to examine various factors influencing the characteristics of the corbels. These factors included the replacement ratio of natural coarse aggregate with varying proportions of RCA, with a replacement ratio of 0 % designed for the reference mixture; the other mixtures had replacement ratios of 20 %,40 %, and 60 %. Additionally, the study assesses the amount of main and secondary reinforcement, the shear span-effective depth ratio (a/d), and compressive strength. The influence of these variables on ultimate load capacity, load-deflection curves, crack pattern, initial stiffness, and energy dissipation was investigated. The results indicated that the use of recycled concrete aggregate did not significantly affect the pattern of cracks, type of failure, and energy dissipation capabilities. At the same time, it had a modest impact on the ultimate load capacity, with a decrease of 4.4 %, 8.6 %, and 16 % at a replacement ratio of 20 %,40 %, and 60 %, respectively. Correspondingly, deflection increased from 3.63 mm to 4.27, 4.92, and 5.61 mm at the same replacement ratio. Furthermore, it was also noted that increasing replacement ratios resulted in a slight decrease in initial stiffness. The ultimate load capacity of the corbels was predicted using the theoretical equations proposed by the provisions of the ACI 318 code and the equations proposed by previous literature. The results indicated that using the equations proposed by Hwang et al. and Chetchotisak et al. provided more accurate estimates compared to the other models, yielding a coefficient of variations (COVs) of 4.8 and 5.1 %, respectively. In contrast, the values derived from the code equations were significantly more conservative.

1. Introduction

The use of recycled aggregate in the production of concrete structures is attaining high research attention in the present time since it contributes in maintaining natural resources on one hand, and reduces the environmental attack of the process of demolishing structures on the other hand. The dark side of the issue is that the use of recycled aggregate often results in concrete of lower strength and elastic properties than concrete using aggregate from natural sources. This is why many research efforts were spent to evaluate the strength and behavior of structural components made of concrete incorporating recycled aggregate [1–4]. In the present work, the use of recycled aggregate as a partial replacement of the natural aggregate in reinforced concrete corbels subjected to vertical load is examined concerning their deflection and crack and failure loads. The utilization of recycled aggregates, encompassing both coarse and fine aggregate types, has been the subject of significant research in recent years. Investigation into these materials has been conducted across various domains within structural engineering [5–15].

Corbels can be thought of as short cantilevers projected from columns or walls and subjected to vertical and horizontal forces from beams resting on them [16]. They are commonly used in workshops with crane girders and other pre-cast reinforced concrete buildings. These elements generally have shear span-depth ratios of less than unity [17]; thus, the classical flexural theory cannot be used to determine their strength. This is because the three-dimensional state of stress in the region between the applied load and the reaction at the support, which makes the assumption of plane section before bending remains plane after bending is no longer valid. So many attempts were made to predict the shear strength of the reinforced concrete corbels by using experimental and analytical studies [18–25]. Among those studies, Campione (2009) [26] studied the flexural behavior of ordinary and fiber-reinforced concrete corbels under vertical and horizontal loads, proposing a strut-and- tie-based analytical model. Key parameters

* Corresponding author.
E-mail address: kadhim.Naser@uobasrah.edu.iq (K.Z. Naser).

https://doi.org/10.1016/j.rineng.2025.104101
Received 25 September 2024; Received in revised form 5 January 2025; Accepted 20 January 2025
Available online 21 January 2025

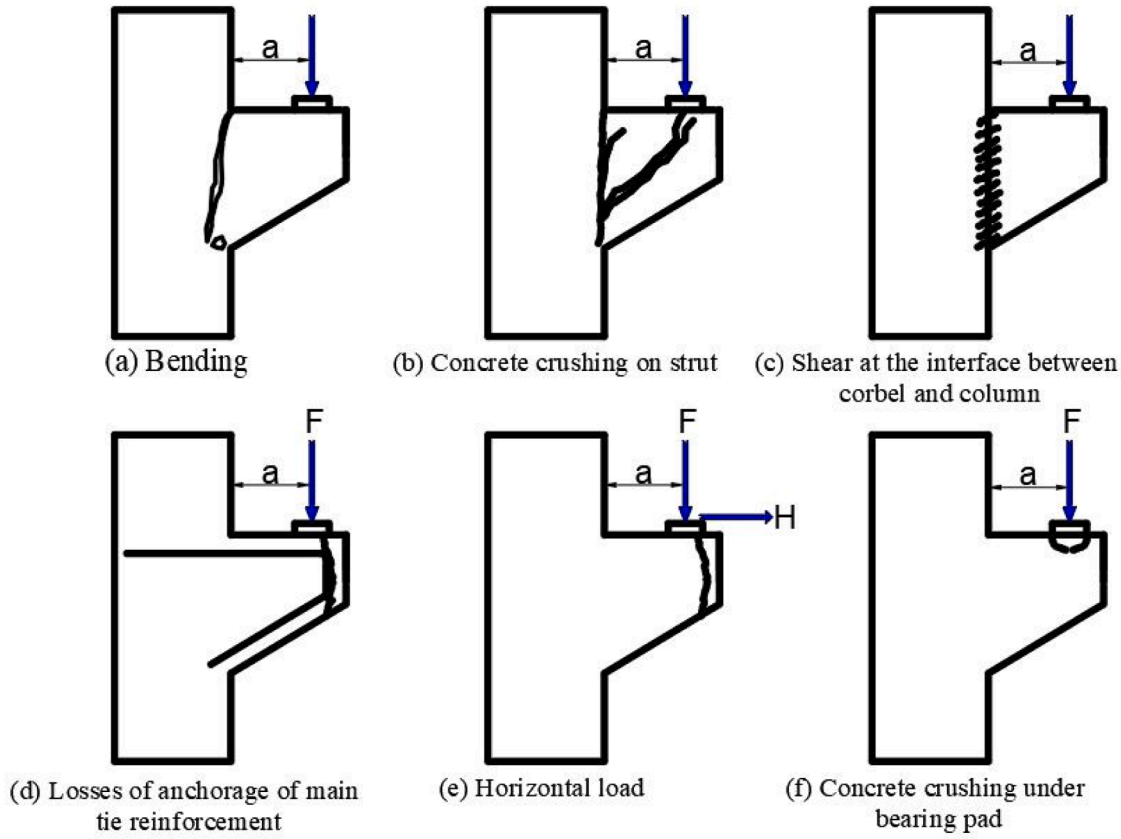

Fig. 1. Modes of failure for corbels adapted from Shakir [42].

included concrete type, the ratio and arrangement of main and secondary reinforcement, and steel fiber ratio. Failure was ductile with low reinforcement and brittle with high reinforcement. In his other paper, Campione (2009) [27] proposed a strut and tie analogy to determine the flexural strength of R.C. corbels, incorporating the use of steel fibers under the action of vertical loading. Abdul-Razzak and Mohammed Ali (2011) [28] developed a constitutive material model for high-strength steel fiber-reinforced concrete using SPSS statistical software, which was subsequently applied it the finite element analysis of concrete corbels. The model incorporated plane stress conditions and strain-hardening plasticity. In their other work [29], the same authors considered the effect of cracks on the strength of nonlinear models of R. C. corbels. Abdel Hafez et al. (2012) [30] experimentally investigated the shear behavior of high-strength concrete corbels, examining steel fiber content, concrete strength, span/depth ratio, and the properties of main and horizontal reinforcement. Steel fibers enhanced the initial stiffness, shear strength, and ductility, with similar improvements observed from increased main reinforcement ratios.

Salman et al. (2014) [31] studied the effect of steel fiber, compressive strength, and shear span/depth (a/d) ratio on self-compacting concrete corbels. Higher (a/d) ratios increased deflection under the same load and reduced cracking and ultimate loads, with greater nonlinearity in the load-deflection response. All the ten specimens failed via diagonal splitting.

There were many works dealing with strengthening the R.C. corbels with carbon fiber-reinforced polymer (CFRP). Ivanova et al. (2015) [32] conducted an experimental program to investigate the effect of the various patterns of CFRP strips. Assih et al. (2015) [33] examine through experimental and theoretical studies the recovered strength of damaged R.C. corbels after rehabilitation using CFRP. Sayhood et al. (2016) [34] and Yassin (2016) [35] experimentally explore the improvement that CFRP can provide to the strength of corbels subjected to monotonic loading. Ivanova and Assih (2016) [36] investigated the behavior of corbels strengthened by CFRP stripes under the action of static and fatigue loading. Al-Kamaki et al. (2018) [37] tested twelve corbel specimens to explore the effect of secondary steel reinforcement and the addition of CFRP sheets on their behavior. They found that adding reinforcement in the mid-height of corbels and CFRP sheets, especially inclined with 45°, both increase the ultimate strength by up to 27 %.

Satish et al. (2017) [38] studied self-compacted concrete with recycled aggregate, finding reduced flowability above a 40 % replacement ratio and decreased strength starting at 20 % replacement ratio. Sulaiman and Khudair (2019) [39] conducted an experimental study to investigate the effect of partial replacement of natural aggregate by recycled one on self-compacting concrete. They found that for a replacement ratio of 25, 50, and 75 %, the strength reductions were about 2.2, 7.4, and 12.3 %, respectively. They also found that the replacement ratio inversely affects both the crack load and mix workability. In their second work, Sulaiman and Khudair (2020) [40] studied the effect of replacement ratio, h/H ratio, and area of horizontal reinforcement on self-compacting concrete corbels. They found brittle failure in corbels without horizontal reinforcement and a 56.5 % higher failure load in rectangular brackets ($h/H = 1.0$) compared to the trapezoidal shape of ($h/H = 0.25$). Hamoodi et al. (2021) [41] investigated the impact of recycled aggregate on deflection, cracking, and failure loads in reinforced concrete corbels, finding that higher replacement ratios and shear-to-depth (a/d) ratios reduce crack and failure loads.

It was reported that there are six common failure modes of R. C. corbels: which are flexure, crushing of concrete on struct, vertical shear failure at column face, slipping of main reinforcement, lateral failure due to horizontal load, and local bearing failure at the interface with the beam [42]. These modes of failure are illustrated in Fig. 1.

Table 1
Chemical and physical properties of cement.

Chemical properties		
Components	Test result Contents (%)	Limits of ASTM C150–19 [43]
CaO	63.11	—
SiO_2	20.5	—
Al_2O_3	5.11	—
Fe_2O_3	4.1	—
MgO	2.46	6.0 (max)
SO3	2.26	—
Loss on Ignition (L.O.I)	2.19	3.0 (max)
Na_2O	0.29	—
K_2O	0.62	—
Insoluble residue	0.51	0.75 (max)
Potential compounds		
C3S	51.9	—
C2S	17.8	—
C3A	2.52	3.0 (max)
C4AF	13.2	25.0 (max)
Physical properties		
Specific surface area (Blaine method) (m^2/kg)	310	Not <280
Setting time (Vicat method) (min)		
Initial setting time	140	>45
Final setting time	295	<375
Compressive strength (MPa)		
3 days	17.2	>12
7 days	23.8	>19
Specific gravity (g/cm^3)	3.15	—
Color	Light grey	—

1.1. Research significance

This study examines the feasibility of employing RCA as a sustainable partial substitute for natural coarse aggregate in concrete production, with the objective of addressing the increasing accumulation of construction and demolition waste. Through the incorporation of RCA, the research seeks to alleviate environmental challenges, decrease reliance on diminishing natural aggregate resources, and foster sustainable construction particles. The investigation emphasizes the mechanical properties and durability of RCA-integrated concrete to identify optimal replacement ratios that achieve a balance between structural performance and sustainability, thereby providing valuable insights for future application within the construction industry. At the same time, limited data exists regarding the behavior of corbels made using RCA as coarse aggregate. To bridge this gap, the current work focuses on exploring the impact of using recycled concrete aggregate as a partial replacement for natural coarse aggregate at replacement ratios of 0 %, 20 %, 40 %, and 60 % on various properties of reinforced concrete corbels under axial load. These properties include ultimate load-carrying capacity (ULC), load-deflection response, initial cracking, diagonal cracking, failure modes, initial stiffness, and energy dissipation capacity. Additionally, the study compares the experimental ultimate load-carrying capacity with ACI 318 provisions and findings from previous literature.

2. Experimental work

2.1. Material characteristics

2.1.1. Cement

The cement utilized in this study is ordinary Portland cement (Type I), Al-Mabrouka type, produced locally in Basra Governorate and conforming to ASTM C150–19 [43] specifications. The chemical and physical properties are presented in Table 1.

2.1.2. Fine aggregate

The natural fine aggregate used in this study is available locally in the Al-Zubair region of Basra Governorate. It was tested according to the ASTM C33–23 [44] standard specification, and the gradation of the fine aggregate is within the limits of this specification. Table 2 presents the gradation and the physical properties of fine aggregate, and the grading curves of the fine aggregate can be seen in Fig. 2.

Table 2
The sieve analysis and physical properties of fine aggregate.

Sieve Size (mm)	Passing (%)	ASTM C33–23 [44]
9.5	100	100
4.75	98	95–100
2.36	91	80–100
1.18	73	50–85
0.6	39	25–60
0.3	11	5–30
0.15	0	0–10
Physical properties		
Specific gravity	2.56	—
Bulk density (kg/m^3)	1680	—
Sulfate content (SO_3) %	0.31	—
Absorption %	1.1	—
Fineness modulus	2.85	—
Maximum particle size (mm)	5	—

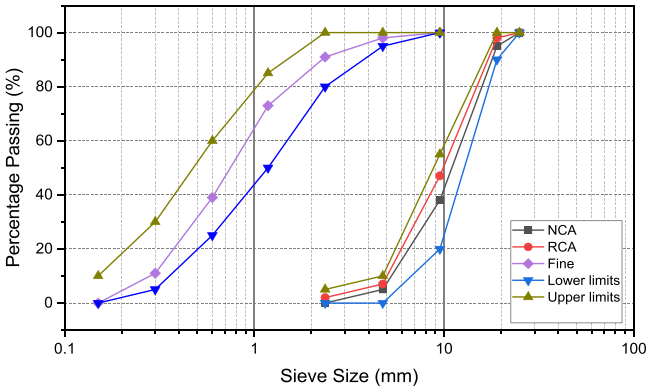

Fig. 2. Grading curves for Coarse and fine aggregates.

Fig. 3. Appearance of coarse aggregates: (a) NCA and (b) RCA.

2.1.3. Coarse aggregate

In this study, two types of coarse aggregate were employed: natural coarse aggregate (NCA) and recycled coarse aggregate (RCA). The natural coarse aggregate employed in this study was sourced from the Safwan region in Basra Governorate. The recycled coarse aggregate was obtained from crushing old concrete cubes and cylinders, which were available in the laboratory and had been there for more than two years. The compressive strength of these cubes and cylinders ranged between (25–40) MPa. Subsequently, the cubes and cylinders were subjected to crushing using a rock crusher machine, transforming the material into granules. The granules retained on a 4.75 mm sieve were then collected. Fig. 3 illustrates the appearance of NCA and RCA.

Table 3
The sieve analysis and physical properties of coarse aggregate.

Sieve Size (mm)	Passing (%)		ASTM C33–23 [44]
	NCA	RCA	
25	100	100	100
19	95	98	90–100
9.5	38	47	20–55
4.75	5	7	0–10
2.36	0	2	0–5
Physical properties			
Specific gravity, Bulk oven- dry	2.61	2.38	—
Bulk specific gravity (SSD)	2.64	2.43	
Loose bulk density (kg/m^3)	1520	1328	—
Water Absorption %	0.7	3.81	—
Maximum particle size (mm)	19	19	—

The bulk density was calculated according to ASTM C29/C29 M [45], while the water absorption and specific gravity of the coarse aggregate were calculated according to ASTM C127–15 [46]. The gradation of natural and recycled aggregate meets the requirements of ASTM C33–23 [44]. It can be observed that the gradation for both types is within the limits of this standard. Table 3 presents the gradation and physical properties of both types, while Fig. 2 shows the gradation curves for natural and recycled coarse aggregate that was used in this work.

2.1.4. Admixture

In this study, a superplasticizer designated as Glunium 54 was employed at a ratio of (0.5 – 1.75) L/100 kg of binder material, in accordance with the manufacture specifications. This superplasticizer complies with the ASTM C494/C494M-19 [47] specifications. It was employed exclusively in high-strength class mixtures.

2.1.5. Steel bars

In this work, conventional steel bars of grade 60 with varying diameters were used. The mechanical specifications of the reinforcing steel are summarized in Table 4. These specifications meet the requirements of ASTM A615–24 [48].

2.1.6. Concrete mixes

The mix designs were prepared in accordance with the specifications outlined in ACI 211.1 [49]. In this study, two types of concrete mixtures were employed: one with normal compressive strength and the other with high compressive strength.

To achieve normal compressive strength, four concrete mixtures were utilized. The first mixture incorporated natural coarse aggregate, while the remaining mixtures incorporated natural coarse aggregate that was partially replaced with recycled coarse aggregate at ratios of 20 %, 40 %, and 60 %. For the high compressive strength, a single mixture was employed in which the natural aggregate was partially replaced with 40 % recycled aggregate. The description and details of the mixes are presented in Tables 5 and 6, respectively.

Following the completion of the concrete mixing process, the slump of concrete was measured in accordance with the provisions of ASTM C143/C143M-20 [50]. Furthermore, to evaluate the compressive strength of each mixture, three cylindrical specimens measuring 300 mm in height and 150 mm in diameter were cast and tested according to ASTM C39/C39M-21 [51]. Additionally, three cubic specimens measuring 150 * 150 *150 mm were prepared and cast, according to BS EN 12,230–19 [52].

Table 5
Mix description.

Mix I.D.	Mix description
NCS 0	Normal Concrete Strength without Recycled Concrete Aggregate.
NCS 20	Normal Concrete Strength with 20 % Recycled Concrete Aggregate.
NCS 40	Normal Concrete Strength with 40 % Recycled Concrete Aggregate.
NCS 60	Normal Concrete Strength with 60 % Recycled Concrete Aggregate.
HCS 40	High Concrete Strength with 40 % Recycle Concrete Aggregate.

Furthermore, to evaluate splitting tensile strength, three cylindrical specimens of the same dimensions were cast and tested according to the ASTM C496–17 [53]. All specimens were demolded after 24 h and subsequently cured until testing at 28 days.

After 24 h, the cast corbels were demolded. Subsequently, they were covered with polyethylene sheets for 48 h to prevent moisture loss. Then, the specimens were stored and treated with water until they were examined.

2.2. RC corbel specimens

The experimental program conducted in this study involved twenty corbels. All dimensions of corbels were 200 mm in width, a total depth of 260 mm, and an effective depth of 230 mm. Corbels with aspect ratios a/d = 0.4 and 0.6 had a length of 250 mm, while those with a/d ratios of 0.8 and 1.0 were 340 mm in length. The columns for all corbels measured 200 * 200 * 510 mm and were reinforced with four bars with a diameter of 12 mm at the corners and ties of 10 mm diameter at equal distances of 110 mm from center to center. The details of the corbels utilized in this study are presented in Fig. 4 and Table 7. Additionally, details of the preparation of the corbel mold, arrangement of steel reinforcement, and casting of the specimens are displayed in Fig. 5.

The twenty specimens were divided into five Groups, each Group containing four corbels, according to the variables studied in this research as follows:

Group A: Investigated the effect of various ratios of recycled aggregate in the concrete mixtures. The replacement ratio (by weight) was taken as 0, 20, 40, and 60 % of natural coarse aggregate.

Groups B and C: Studied the influence of various ratios of secondary A_h and main steel reinforcement A_{sc}, respectively.

Groups D and E: examined different ratios of a/d with ratios of 0.4, 0.6, 0.8, and 1 for normal and high compressive strength, respectively.

2.3. Corbels design and test setup

To test the corbel samples, they were placed in an inverted position to apply the load to the upper end of the column, which was covered with a steel plate with dimensions of (200×200×40) mm to distribute the load uniformly on the specimens. The specimens were supported symmetrically at the outer edges on steel supports. The location of these supports is variable, depending on the shear span distance (a). These supports comprise bearing plates with dimensions of (400 * 70 * 30) mm, which are in direct contact with the horizontal surface of the corbels. The loads were applied to the specimens using the universal loading machine UTM with a capacity of 2000 kN, as illustrated in Fig. 6.

The load was transferred to the data acquisition system by installing

Table 4
Properties of reinforcing bars.

Nominal diameter (mm)	Measured diameter (mm)	Surface texture	Area (mm^2)	f_y (MPa)	f_u (MPa)	Elongation (%)
8	8	deformed	50.24	485	651	12.9
10	10	deformed	78.5	451	598	12.2
12	12	deformed	113	472	632	11.9
16	16	deformed	201	467	612	11.7

Table 6
Concrete mix proportions (kg/m3).

Mix I.D.	RCA replacement ratio (%)	Cement (kg/m^3)	Water (Liter)	Sand (kg/m^3)	Natural coarse aggregate (kg/m^3)	Recycled coarse aggregate (kg/m^3)	S.P. (Liter)
NCS 0	0	430	195	690	1090	0	0
NCS 20	20	430	195	690	872	218	0
NCS 40	40	430	195	690	654	436	0
NCS 60	60	430	195	690	436	654	0
HCS 40	40	520	190	800	540	360	5.2

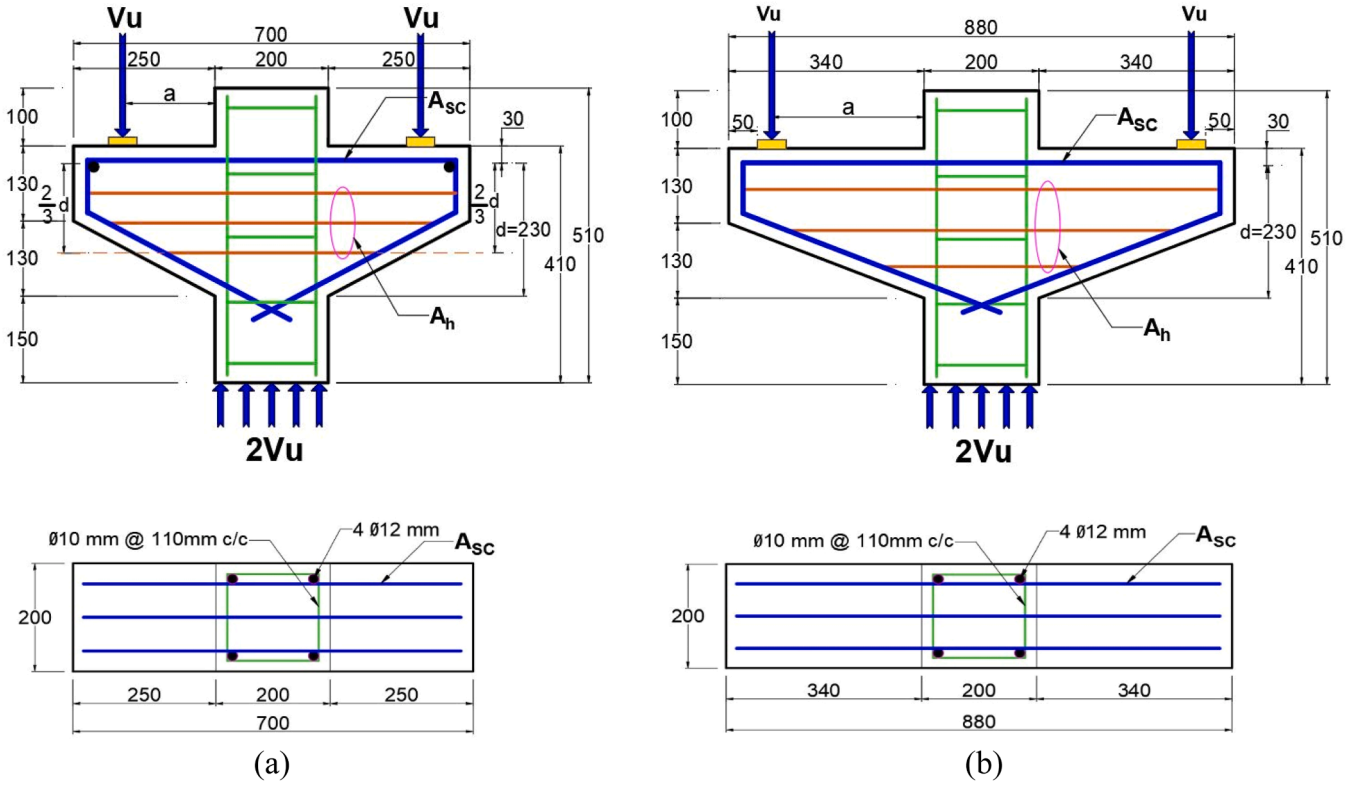

Fig. 4. Corbels details: (a) for a/d = 0.4 and 0.6, and (b) for a/d = 0.8 and 1.0, all dimensions in mm.

Table 7
Details of corbel specimens.

Group	Corbel designation	Type of Concrete	a/d	Main reinforcement (A_{sc})	Horizontal stirrups (A_h)
A	CA1 – 0 R- Control	NCS 0	0.4	3-Ø12mm	2-Ø8 mm
	CA2 - 20 R	NCS 20	0.4	3-Ø12mm	2-Ø8mm
	CA3 - 40 R	NCS 40	0.4	3-Ø12mm	2-Ø8mm
	CA4 - 60 R	NCS 60	0.4	3-Ø12mm	2-Ø8mm
B	CB1 – 40 R Control	NCS 40	0.4	3-Ø12mm	—-
	CB2 – 40 R	NCS 40	0.4	3-Ø12mm	2-Ø 8mm
	CB3 40 R	NCS 40	0.4	3-Ø12mm	3-Ø 8mm
	CB4 40 R	NCS 40	0.4	3-Ø12mm	4-Ø 8mm
C	CC1 – 40 R Control	NCS 40	0.4	3-Ø10mm	2-Ø8mm
	CC2 – 40 R	NCS 40	0.4	3 -Ø 12mm	2-Ø8mm
	CC3 40 R	NCS 40	0.4	2-Ø16mm	2-Ø8mm
	CC4 40 R	NCS 40	0.4	4-Ø12mm	2-Ø8mm
D	CD1 – 40 R - Control	NCS 40	0.4	3-Ø12mm	2-Ø8mm
	CD2 – 40 R	NCS 40	0.6	3-Ø12mm	2-Ø8mm
	CD3 40 R	NCS 40	0.8	3-Ø12mm	2-Ø8mm
	CD4 40 R	NCS 40	1.0	3-Ø12mm	2-Ø8mm
E	CE1 – 40 R - Control	HCS 40	0.4	3-Ø12mm	2-Ø8mm
	CE2 – 40 R	HCS 40	0.6	3-Ø12mm	2-Ø8mm
	CE3 40 R	HCS 40	0.8	3-Ø12mm	2-Ø8mm
	CE4 40 R	HCS 40	1.0	3-Ø12mm	2-Ø8mm

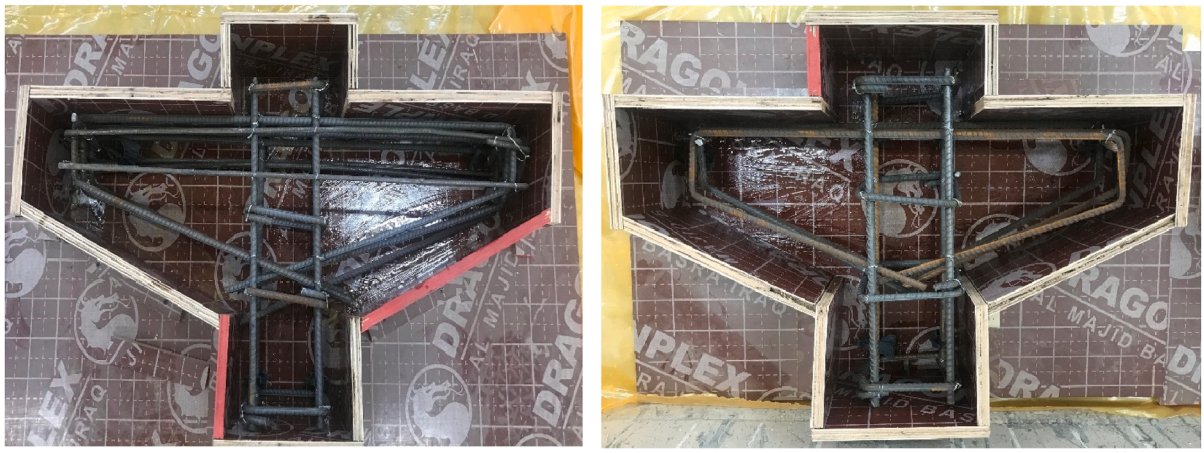

(a)

(b)

Fig. 5. Preparation of corbels (a) formwork and reinforcement arrangement; and (b) casted specimens.

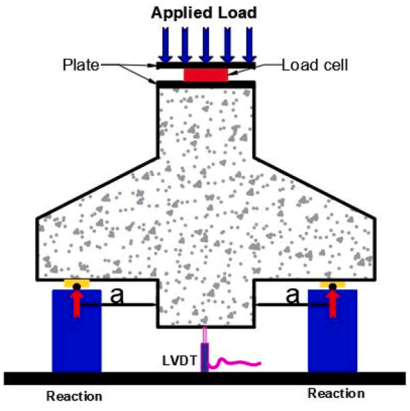

Fig. 6. Test setup.

a load cell below the hydraulic jack and above the column. To measure the vertical displacement, a linear variable displacement transducer (LVDT) was used in the center of the column from the bottom, enabling the direct recording of the load increase and the corresponding displacement in the data logger.

The design of the corbels was based on the American Concrete Institute (ACI) 2019 [54] standards and included the following considerations : (a) the dimensions were established in accordance with

Table 8
Results of fresh and hardened concrete mixtures.

Mix I.D.	RA replacement ratio (%)	Slump (mm)	Compressive strength (f_{cu}) (MPa) At 28 days	Compressive strength (f'_c) (MPa)	Splitting tensile strength (MPa)
NCS 0	0	96	37.6	32.8	3.35
NCS 20	20	94	36.2	31.1	3.22
NCS 40	40	93	34.8	29.4	3.11
NCS 60	60	92	32.4	28.2	3.03
HCS 40	40	100	51.7	46.7	3.91

Section 16.5.2.4 of the ACI 2019 standard; (b) the reinforcement arrangement followed the specifications in Section 23.5.1 to 23.5.5 of the ACI 2019 standard, with additional guidance from Figures R16.5.1.b and R23.5.1; and (c) the shear span -to- effective depth ratio (a/d) was calculated using the provisions in Section 16.5.1.1 of the ACI 2019 standard.

3. Results and discussion

3.1. Properties of fresh and hardened concrete mixtures

3.1.1. Slump

The results of the properties of fresh and hardened concrete for all mixtures are presented in Table 8. As can be observed from the data presented in the table, the slump measurements for all mixtures exhibited a notable degree of similarity, and this is consistent with the findings of [55,56]. This is due to the fact that both types of aggregates are in a dry saturated surface state (SSD). Consequently, the water-to-cement ratio did not consider the water absorbed by the saturated aggregate. This is to ensure that there is approximately the same amount of remaining water, which is sufficient to ensure the hydration of the cement particles in the concrete mixture. This approach has been adopted by several previous works [14,41,57–59].

3.1.2. Compressive strength

The compressive strength of the specimens was evaluated on the same day as the corbel test at 28 days. The results of the compressive strength test are presented in Table 8. The results given in Table 8 indicate that an observed decrease in compressive strength was associated with an increase in the replacement ratio of the recycled aggregate, this result was also identified by [60–69]. The amount of the decrease was 5.2, 10.4, and 14.0 % for the replacement ratios of 20, 40, and 60 %, respectively in the normal compressive strength category. Consequently, the reduction in compressive strength of 10.4 % observed for the 40 % replacement ratio of natural aggregate with recycled aggregate is relatively minor in comparison to the 60 % replacement ratio, where the reduction was 14.0 %.

One significant drawback of RCA is the presence of microcracks formed during the crushing process, which converts concrete block into coarse aggregate particles [70–72], to thoroughly assess the effect of RCA under high-strength conditions, the study incorporated both high-compressive -strength and normal – strength concrete samples. This dual approach allowed for the elevation of RCA impact on the performance of reinforced concrete corbels across a spectrum of compressive strength a more comprehensive understanding of RCA behavior under varying conditions, thereby expanding knowledge on its use in structural applications

3.1.3. Splitting tensile strength

To evaluate the splitting strength of recycled concrete, the test was performed on concrete cylinders tested on the same day as the corbel test at 28 days. The test results are presented in Table 8. The data presented in the table demonstrates that an increase in the replacement ratio results in a slight decrease in splitting strength, particularly at low levels 20 and 40 % of the replacement ratio. This result is consistent with previous research [68,69,73–75].

This indicates that recycled concrete has a lower splitting strength than conventional concrete; however, it has sufficient structural integrity to be used in concrete structures [69].

Table 9
Experimental results of the ultimate load capacity.

Group	Corbel designation	Type of Concrete	P_u(kN)	Change in P_u (%)
A	CA1 – 0 R- Control	NCS 0	712	–
	CA2 - 20 R	NCS 20	681	−4.4*
	CA3 - 40 R	NCS 40	651	−8.6
	CA4 - 60 R	NCS 60	598	−16.0
B	CB1 – 40 R Control	NCS 40	412	–
	CB2 – 40 R	NCS 40	531	28.9
	CB3 40 R	NCS 40	655	59.0
	CB4 40 R	NCS 40	695	68.7
C	CC1 – 40 R Control	NCS 40	583	–
	CC2 – 40 R	NCS 40	661	13.4
	CC3 40 R	NCS 40	702	20.4
	CC4 40 R	NCS 40	771	32.2
D	CD1 – 40 R - Control	NCS 40	647	–
	CD2 – 40 R	NCS 40	511	−21.0
	CD3 40 R	NCS 40	413	−36.2
	CD4 40 R	NCS 40	343	−47.0
E	CE1 – 40 R - Control	HCS 40	786	–
	CE2 – 40 R	HCS 40	681	−13.4
	CE3 40 R	HCS 40	532	−32.3
	CE4 40 R	HCS 40	443	−43.6

Note: * Minus sign refers to the decreasing percentage.

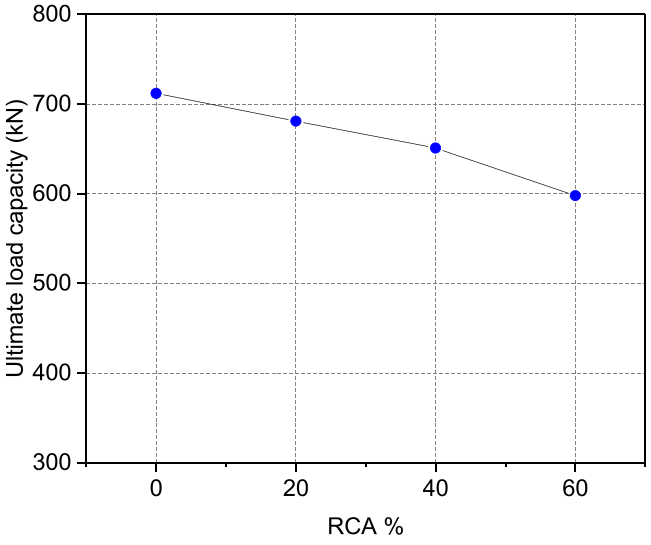

Fig. 7. Effect of various ratios of RCA on ultimate load capacity for Group A.

3.1.4. Ultimate load capacity of corbels

The ultimate load capacity (P_u) of the corbels was recorded and presented in Table 9. As illustrated in Table 9, the ultimate load capacity of Group A declines as the replacement ratio of recycled aggregate increases. The reduction rates were 4.4, 8.6, and 16 % for replacement ratios of 20,40 and 60 %, respectively, as displayed in Fig. 7. This finding has been identified by other researchers [62,76–78].

The reduced ultimate load capacity (P_u) of reinforced concrete corbels incorporating high percentages of recycled concrete materials is attributed to several factors: (a) the weaker Interfacial Transition Zone

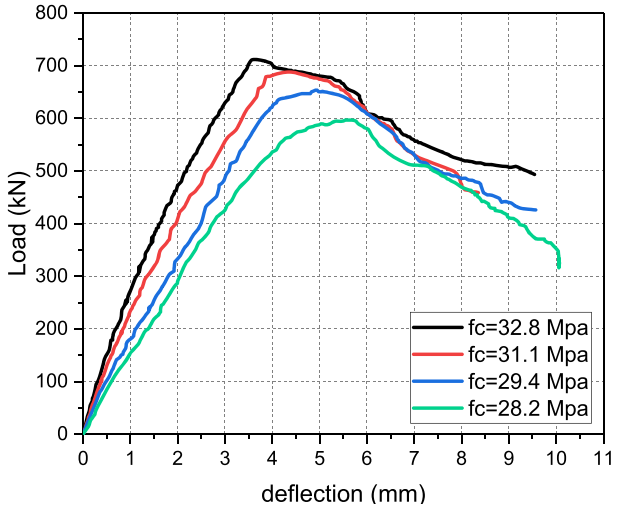

Group (a)

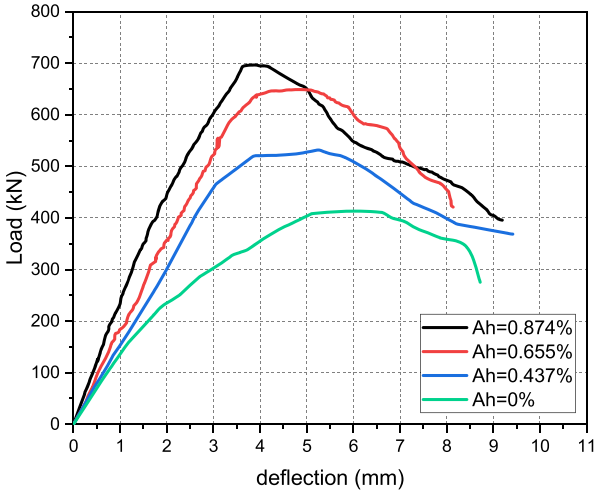

Group (b)

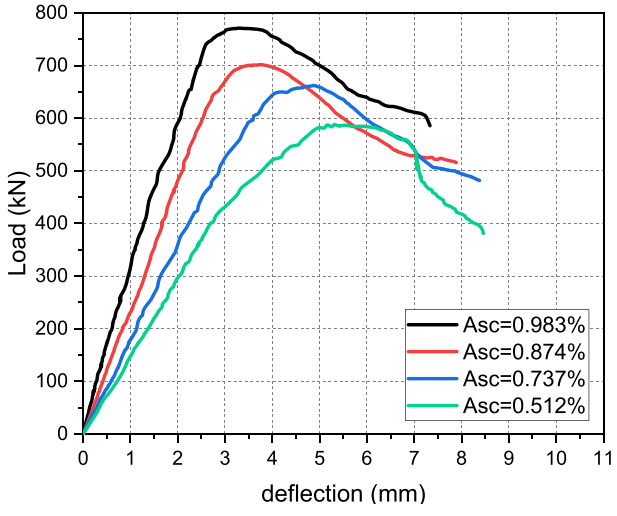

Group (c)

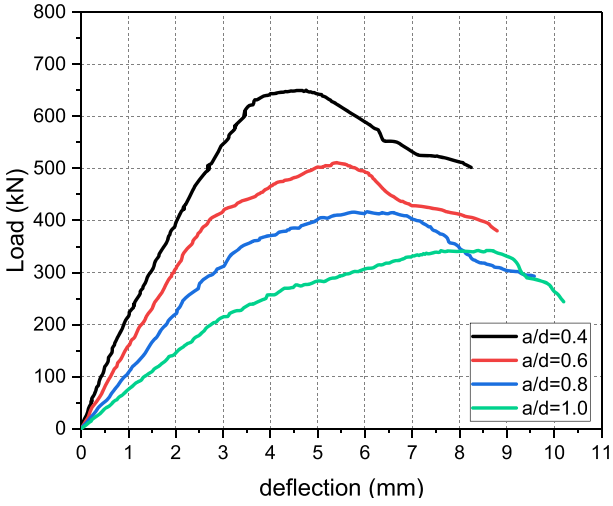

Group (d)

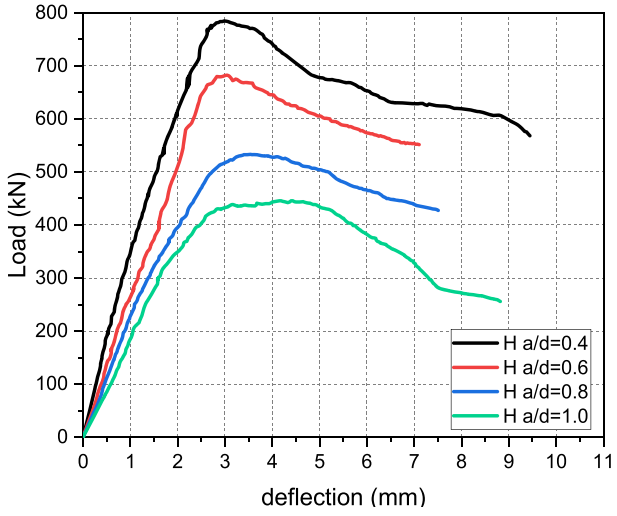

Group (e)

Fig. 8. Load deflection curves of tested corbels.

Table 10
Characteristics of the load–displacement relationship.

Group	Corbel designation	P_u(kN)	Δ_u (mm)	Change in Δ_u (%)	$P_{cr\text{-}flex}$ (kN)	$P_{cr\text{-}diag.}$ (kN)	Failure modes**
A	CA1 – 0 R- Control	712	3.63	–	142	364	SF
	CA2 - 20 R	681	4.27	17.6	124	302	SF
	CA3 - 40 R	651	4.92	35.5	105	266	SF
	CA4 - 60 R	598	5.61	54.5	92	223	SF
B	CB1 – 40 R Control	412	6.35	–	61	143	SF
	CB2 – 40 R	531	5.26	−17.2*	95	207	SF
	CB3 40 R	655	4.88	−23.1	108	296	SF
	CB4 40 R	695	3.83	−39.7	152	342	SF
C	CC1 – 40 R Control	583	5.32	–	83	205	SF
	CC2 – 40 R	661	4.87	−8.5	104	312	SF
	CC3 40 R	702	3.77	−29.1	122	359	SF
	CC4 40 R	771	3.32	−37.6	159	411	SF
D	CD1 – 40 R - Control	647	4.63	–	112	279	SF
	CD2 – 40 R	511	5.36	15.8	83	215	SF
	CD3 40 R	413	6.21	34.1	72	141	DS
	CD4 40 R	343	8.73	88.6	55	98	DS
E	CE1 – 40 R - Control	786	2.95	–	168	425	SF
	CE2 – 40 R	681	3.26	10.5	135	328	SF
	CE3 40 R	532	3.84	30.2	98	208	DS
	CE4 40 R	443	4.35	47.5	79	123	DS

Note: * Minus sign refers to the decreasing percentage; ** Failure modes, SF is Shear Failure, and DS is Diagonal Shear Failure.

(ITZ) between recycled aggregate and residual mortar diminishes bond strength [79–81]; (b) the lower compressive strength of recycled concrete aggregate (RCA), especially at high replacement ratios, directly impacts load-carrying capacity as compressive strength is essential for structural performance [82,83]; (c) microcracks formed during the crushing of old concrete further weaken the material under applied loads [71,84]; (d) increased porosity and water absorption due to retained old mortar reduce the overall strength and durability of the concrete [84–86]; (e) the weaker matrix and interfacial zones in recycled aggregate concrete, which reduce the bond strength between steel reinforcement and surrounding concrete, impairing the composite action necessary for effective structural performance [87–89]; and (f) variability in the quality of recycled aggregates, often due to diverse sources, leads to inconsistencies in the mechanical properties of the concrete, exacerbating its limitations [90,91].

The 8.6 % decrease in ultimate load capacity observed at a 40 % replacement ratio is relatively minor, especially considering the significant amount of concrete waste recycled to produce reinforced concrete corbels. The findings identified a 40 % replacement ratio as an optimal compromise, maximalizing the use of recycled concrete aggregate (RCA) while thoroughly assessing its impact on the structure performance of reinforced concrete. The study concluded that incorporating RCA at this level had minimal effect on the overall structural behavior if reinforced concrete corbels. This slight reduction in performance is considered acceptable given the substantial environmental advantages, such as sustainable concrete waste management and the promotion of eco-friendly construction practices. Furthermore, the essential engineering properties required for reinforced concrete corbels were adequately preserved.

In Group B, it was observed that an increase in the secondary reinforcement ratio from 0 % to 0.437, 0.655, and 0.874 % led to a corresponding increase in the ultimate load capacity of 28.9, 59.0, and 68.7 %, respectively. Similarly, in Group C, an increase in the main reinforcement ratio from 0.512 to 0.737, 0.874, and 0.983 % resulted in a notable enhancement in the ultimate load capacity of 13.4, 20.4, and 32.2 %, respectively. It was observed that the ultimate load capacity decreased as the a/d ratio increased. The amount of decrease was 21.0, 36.2, and 47.0 % for Group D, while for Group E, the reductions were 13.4, 32.3, and 43.6 % as the a/d ratio increased from 0.4 to 0.6, 0.8, and 1.0, respectively. These results are displayed in Table 9. This is consistent with the findings from other researchers who have employed natural aggregate to investigate the properties of corbels [92–97].

Hence, it can be concluded that the utilization of 40 % recycled concrete waste had a marginal impact on the general behavior of the corbel, especially when compared to the quantity of waste that can be discarded in order to achieve environmentally friendly concrete.

3.2. Load-deflection response

The load-deflection curves are presented in Fig. 8 and Table 10. Fig. 8 (a) illustrates the impact of the RCA replacement ratio on deflection. As is evident from the figure, an increase in the replacement ratio is accompanied by an increase in the deflection. These results are consistent with those previously documented by other researchers [77, 98–101]. As presented in Table 10, the deflection (Δ_u) reached 3.63 mm at the ultimate load capacity for corbels with 0 % RCA, while the deflection increased to 4.27 mm (17.6 %), 4.92 mm (35.5) and 5.61 mm (54.5 %) at the replacement ratio of 20, 40, and 60 %, respectively. This increase in deflection is attributable to the reduction in stiffness associated with the increase in the replacement ratio.

Figs. 8(b) and 8(c), illustrate the load-deflection curve for various ratios of secondary and main reinforcement, respectively. It was observed that the deflection decreased with an increase in both the secondary and main reinforcement ratio. The enhancement percentages were 17.2, 23.1, and 39.7 %, as the secondary reinforcement ratio increased from 0 % to 0.437, 0.655, and 0.874 % respectively. In contrast, the enhancements were 8.5, 29.1, and 37.6 % when the main reinforcement ratio increased from 0.512 to 0.737, 0.874, and 0.983, respectively. The influence of secondary and main reinforcement on the load-deflection curve was apparent. Therefore, the quantities of both secondary and main reinforcement were established in accordance with the ACI Code [54], paragraphs 16.5.5.1 and 16.5.5.2. The quantity of main reinforcement (A_{sc}) shall be at least the greatest of (a) through (c):

(a) $A_f + A_n$
(b) $(2/3)A_{vf} + A_n$
(c) $0.04(\acute{f}_c'/f_y)(b_w d)$

While the quantity of secondary reinforcement must be not less than the following value:

$$A_h = 0.5(A_{sc} - A_n)$$

Where :
A_f : area of reinforcement resisting design moment, mm^2.
A_{vf} : area of shear-friction reinforcement, mm^2.
A_n : area of reinforcement in resisting factored restraint horizontal

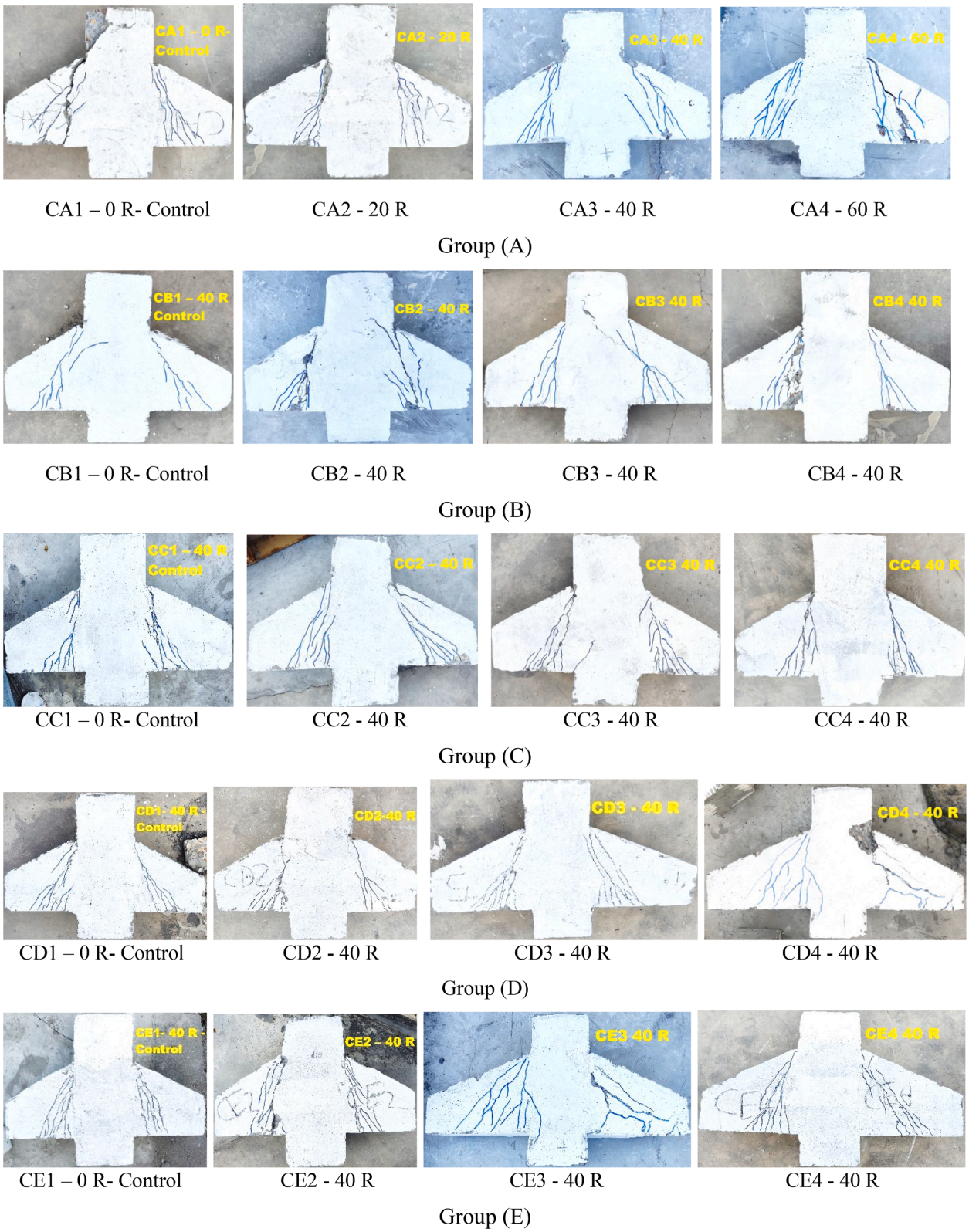

Fig. 9. Crack patterns at failure of tested corbels.

force N_{uc}, mm^2.

A_{sc} : area of primary tension reinforcement, mm^2.

A_h : total area of shear reinforcement parallel to primary tension reinforcement, mm^2.

Figs. 8(d) and 8(e) illustrate the effect of increasing the a/d ratio for the normal strength class of Group D and the high strength class of Group E, respectively. It was observed that the maximum deflection increased with increasing a/d ratio for both Groups. The amount of increase was 15.8, 34.1, and 88.6 % for Group D, while it was 10.5, 30.2, and 47.5 % for Group E when the a/d ratio increased from 0.4 to 0.6, 0.8. 1.0 respectively. In addition, it is noted that the amount of increase in deflection was less at high compressive strength. Thus, when the

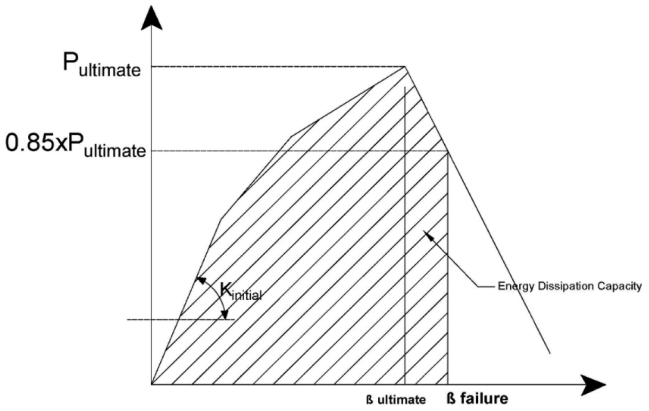

Fig. 10. Method used to calculate initial stiffness and energy dissipation capabilities.

compressive strength increased from 29.4 MPa (NSC40) to 46.7 MPa (HSC40), the deflection improved by 36.3 %, with the replacement ratio and the a/d ratio remaining constant at 40 % and 0.4, respectively.

3.3. Cracking patterns and failure modes

Fig. 9 presents the crack pattern observed at the failure of the tested corbels. It was observed that all specimens exhibited the same response until the point of failure. In the initial stages of loading, approximately (12–17) % of the ultimate load capacity, cracks began to appear. These were flexural cracks ($\boldsymbol{P_{cr\text{-}flex}}$) that extended from the column-corbels face, and as loading increased, the crack grew vertically at a slow rate. As the loads approached approximately (30–40) % of the ultimate load capacity, diagonal cracks ($\boldsymbol{P_{cr\text{-}diag.}}$) began to appear near the load plates; these cracks subsequently widened and continued to grow in width. Furthermore, it was observed that the load tends to transfer directly to the column support, resulting in the formation of diagonal cracks. Thus principle is consistent with the elastic flow of forces [97].

It can be observed that the crack load in the samples with $a/d = 0.4$ and 0.6 was greater than that of the samples with $a/d = 0.8$ and 1.0. Additionally, the formation of flexural cracks was observed to be more delayed in the samples with $a/d = 0.4$ and 0.6 in comparison to the samples with $a/d = 0.8$ and 1.0. For specimens with $a/d = 0.6$, 0.8, and 1.0, the appearance of flexural and diagonal cracks is accelerated as a/d increases. This is due to the increase in tensile tie stresses when the shear span increases, which leads to the formation of cracks. [97].

As illustrated in Fig. 9, the failure pattern observed in corbels containing recycled aggregate is similar to that observed in corbels with natural aggregate. This finding has been identified by other researchers [60,62,73,101,102]; the observed differences were limited to the initial and the diagonal crack load; furthermore, specimens containing recycled aggregate exhibited accelerated initial and diagonal cracks formation, as illustrated in Table 10, which displays the flexural or (initial) crack loads ($P_{cr\text{-}flex.}$), diagonal crack load ($P_{cr\text{-}daig.}$), and the failure mode.

Hence it can concluded that the incorporation of RCA significantly influences the cracking behavior of reinforced concrete corbels in several ways: (a) corbels containing RCA tend to crack at lower loads due to weaker Interfacial Transition Zone (ITZ) and the reduced tensile strength of recycled aggregate [78]; (b) crack in these corbels propagate more rapidly and are often wider, which is attributed to the higher porosity and microcrack density of the recycled aggregate [103]; (c) post-crack ductility is reduced compared to corbels made with natural aggregates, thereby limiting their ability to redistribute stresses effectively [76]; and (d) the combination of ductility and increased brittleness diminishes their capacity to resist extreme loads, such as those indicated seismic activity, rendering corbels containing RCA less suitable for critical applications without appropriate reinforcement and design measures [76]. Nevertheless, with suitable design strategies, material enhancements, and optimal replacement ratios (e.g., 20 %−40 %), the adverse effects of RCA can be mitigated, highlighting its potential as sustainable materials for appropriate construction applications.

3.4. Initial stiffness and energy dissipation capacity

The initial stiffness of the tested specimens is represented by the slope of the linear segment in the initial region of the load-displacement graphs. While the energy dissipation capabilities are represented by the area under the load-displacement curve up to the point of collapse, which is defined as the point at which the load decreases by 15 % after reaching the ultimate load, as illustrated in Fig. 10. This method for calculating initial stiffness and energy dissipation capabilities was adopted from the work of [104–106].

Table 11 presents the initial stiffness values and energy dissipation

Table 11
Results of Initial stiffness and Energy dissipation capacity of corbels.

Group	Corbel designation	Type of Concrete	Initial stiffness (kN/mm)	Change in Initial stiffness (%)	Energy dissipation capacity (kN-mm)	Change in Energy dissipation (%)
A	CA1 – 0 R- Control	NCS 0	288.2	–	3112	–
	CA2 - 20 R	NCS 20	237.0	−17.8*	3185	2.3
	CA3 - 40 R	NCS 40	180.8	−37.3	2973	−4.5
	CA4 - 60 R	NCS 60	145.2	−49.6	2989	−4.0
B	CB1 – 40 R Control	NCS 40	125.2	–	2172	–
	CB2 – 40 R	NCS 40	150.4	20.1	2662	22.6
	CB3 40 R	NCS 40	175.2	39.9	2929	34.9
	CB4 40 R	NCS 40	241.5	92.9	2937	35.2
C	CC1 – 40 R Control	NCS 40	145.6	–	2719	–
	CC2 – 40 R	NCS 40	179.9	23.5	2980	9.6
	CC3 40 R	NCS 40	238.4	63.7	3067	12.8
	CC4 40 R	NCS 40	327.9	125.1	3538	30.1
D	CD1 – 40 R - Control	NCS 40	186.9	–	2946	–
	CD2 – 40 R	NCS 40	157.1	−15.9	2471	−16.1
	CD3 40 R	NCS 40	111.3	−40.5	2384	−19.1
	CD4 40 R	NCS 40	73.0	−61.0	2207	−25.1
E	CE1 – 40 R - Control	HCS 0	392.2	–	3681	–
	CE2 – 40 R	HCS 40	280.1	−28.6	3131	−14.9
	CE3 40 R	HCS 40	227.4	−42.0	2807	−23.7
	CE4 40 R	HCS 40	189.4	−51.7	2291	−37.8

Note: * Minus sign refers to the decreasing percentage.

Table 12
Comparison of experimental and theoretical ultimate load capacity values.

Group	Corbel designation	P_u (kN)	ACI		Hwang et al. (kN)	Russo et al. (kN)	Chetchotisak et al. (kN)	Li et al. (kN)	P_u/P_{SF} (%)	P_u/P_{STM} (%)	P_u/P_{hwang} (%)	P_u/P_{Russo} (%)	$P_u/P_{Chetchotisak}$ (%)	P_u/P_{Li} (%)
			SF (kN)	STM (kN)										
A	CA1 – 0 R-Control	712	545.0	519.1	627.2	674.3	582.3	602.3	1.31	1.37	1.14	1.06	1.22	1.18
	CA2 - 20 R	681	532.5	519.1	619.4	656.1	569.2	577.5	1.28	1.31	1.10	1.04	1.20	1.18
	CA3 - 40 R	651	520.0	519.1	606.0	637.2	555.8	552.4	1.25	1.25	1.07	1.02	1.17	1.18
	CA4 - 60 R	598	511.2	518.9	586.3	623.5	546.1	534.5	1.17	1.15	1.02	0.96	1.10	1.12
B	CB1 – 40 R - Control	412	448.0	432.8	369.5	458.7	384.3	331.4	0.92	0.95	1.11	0.90	1.07	1.24
	CB2 – 40 R	531	520.0	432.8	467.3	548.4	469.6	398.0	1.02	1.23	1.14	0.97	1.13	1.33
	CB3 40 R	655	520.0	519.1	606.0	638.1	555.8	552.4	1.26	1.26	1.08	1.03	1.18	1.19
	CB4 40 R	695	520.0	519.1	606.0	727.8	640.2	552.4	1.34	1.34	1.15	0.95	1.09	1.26
C	CC1 – 40 R Control	583	515.6	351.1	524.9	586.8	506.4	476.8	1.13	1.66	1.11	0.99	1.15	1.22
	CC2 – 40 R	661	520.0	519.1	606.0	637.2	555.8	624.5	1.27	1.27	1.09	1.04	1.19	1.06
	CC3 40 R	702	520.0	541.0	649.3	663.9	581.3	670.4	1.35	1.30	1.08	1.06	1.21	1.05
	CC4 40 R	771	520.0	541.0	680.4	682.8	600.5	703.4	1.48	1.43	1.13	1.13	1.28	1.10
D	CD1 – 40 R - Control	647	520.0	519.1	606.0	637.2	555.8	624.5	1.24	1.25	1.07	1.02	1.16	1.04
	CD2 – 40 R	511	496.1	381.1	426.6	543.9	448.9	443.9	1.03	1.34	1.20	0.94	1.14	1.15
	CD3 40 R	413	372.1	301.0	348.4	472.4	376.9	350.7	1.11	1.37	1.19	0.87	1.10	1.18
	CD4 40 R	343	297.7	248.8	311.0	415.0	323.5	296.9	1.15	1.38	1.10	0.83	1.06	1.16
E	CE1 – 40 R - Control	786	647.3	519.1	676.5	796.3	679.8	749.9	1.21	1.51	1.16	0.99	1.16	1.05
	CE2 – 40 R	681	509.9	381.1	547.1	687.1	554.5	536.7	1.34	1.79	1.24	0.99	1.23	1.27
	CE3 40 R	532	382.4	301.0	472.8	600.9	467.4	423.4	1.39	1.77	1.13	0.89	1.14	1.26
	CE4 40 R	443	306.0	248.8	422.9	530.1	402.0	358.4	1.45	1.78	1.05	0.84	1.10	1.24
	Mean								1.2	1.4	1.1	1.0	1.2	1.2
	Standard deviation (SD)								0.1	0.2	0.1	0.1	0.1	0.1
	Coefficient of variations (COVs) %								11.7	15.8	4.8	8.1	5.1	7.2

capacities. As can be observed from this table, initial stiffness decreases as the replacement ratio increases, as is evident in Group A. This is due to a decrease in compressive strength as the replacement ratio increases, with a reduction of 17.8, 37.3, and 49.6 % at 20, 40, and 60 % replacement ratios, respectively.

An improvement in initial stiffness was observed with an increased ratio of secondary and main reinforcement, as demonstrated in Groups B and C. Conversely, a decrease in initial stiffness was evident with an increased ratio of (a/d), as demonstrated in Groups D and E. Regarding energy dissipation capabilities, the degree of change was minimal, and no discernible variation was observed as a result of changes in replacement ratios. Consequently, the utilization of recycled aggregates does not influence the energy dissipation estimates. These findings are consistent with those reported by [102].

The minimal change in energy dissipation observed at low to moderate replacement ratio of recycled concrete aggregate (RCA) is attributed to several factors: (a) concrete with RCA retains comparable compressive strength and elastic modulus to natural aggregate concrete (NCA), ensuring similar energy dissipations [107,108]; (b) micro-cracks in RCA improve frictional damping during cyclic loading, counteracting any potential reductions [71,109]; (c) energy dissipation is predominantly governed by the steel reinforcement, which remain unaffected by RCA replacement [58,73]; and (d) at low to moderate RCA ratios, the behavior of the concrete is largely influence by the natural aggregates, minimizing the impact of RCA.

4. Comparing experimental results with theoretical equations

Numerous models have been proposed to estimate the ultimate load capacity (ULC) of reinforced concrete corbels made of normal and high-strength concrete. These models include the American code ACI - 2019, as well as empirical equations proposed by various researchers to estimate the strength of corbels. To evaluate these mathematical equations and apply them to corbels made from recycled concrete, this study will discuss the experimental results obtained herein in comparison with the results derived from the empirical equation provided by standard codes and those reported in the existing literature as follows:

1. American Standard Code ACI 318 - 2019 [54]
   This standard employs two methods to estimate the ultimate load capacity (ULC) of corbels. The first method is the Shear Friction Method (SF), detailed in Chapter 16, while the second method is the Strut-and-Tie Method (STM), described in Chapter 23 of ACI 318–2019 [54].
2. Hwang et al. 2017 [110,111]
   Hwang et al. developed a method known as the Softened Strut-and-Tie Model (SSTM), which was utilized to estimate the ultimate load capacity (ULC) of the RC corbels.
3. Russo et al. 2006 [112]
   In 2006, Russo et al. introduced a mathematical model for estimating the ULC of RC corbels.
4. Chetchotisak et al. (2022) [113]
   In 2022, Chetchotisak et al. (2022) developed a model known as the Modified Interactive Strut-and-Tie model (MISTM (to estimate the ultimate load capacity ULC of corbels. This method is based on two distinct mechanisms: the diagonal strut mechanism and the truss mechanism [113].
5. Li et al. (2023) [114]
   Lee et al. (2023) introduced a modified model known as Modified Strut-and-Tie Model (MSSTM) to estimate the ultimate load capacity ULC of corbels. This model is based on the horizontal and diagonal mechanisms of reinforced concrete corbels with and without strengthened steel fibers [114].

Table 12 presents a comparison of the experimental results with the values calculated using theoretical equations. As illustrated in the provided table, the prediction of ultimate load capacity using methods (SSTM) developed by Hwang et al. 2017 and (MISTM) proposed by Chetchotisak et al. (2022) show the best convergence between the experimental results and those estimated using the equations, with the

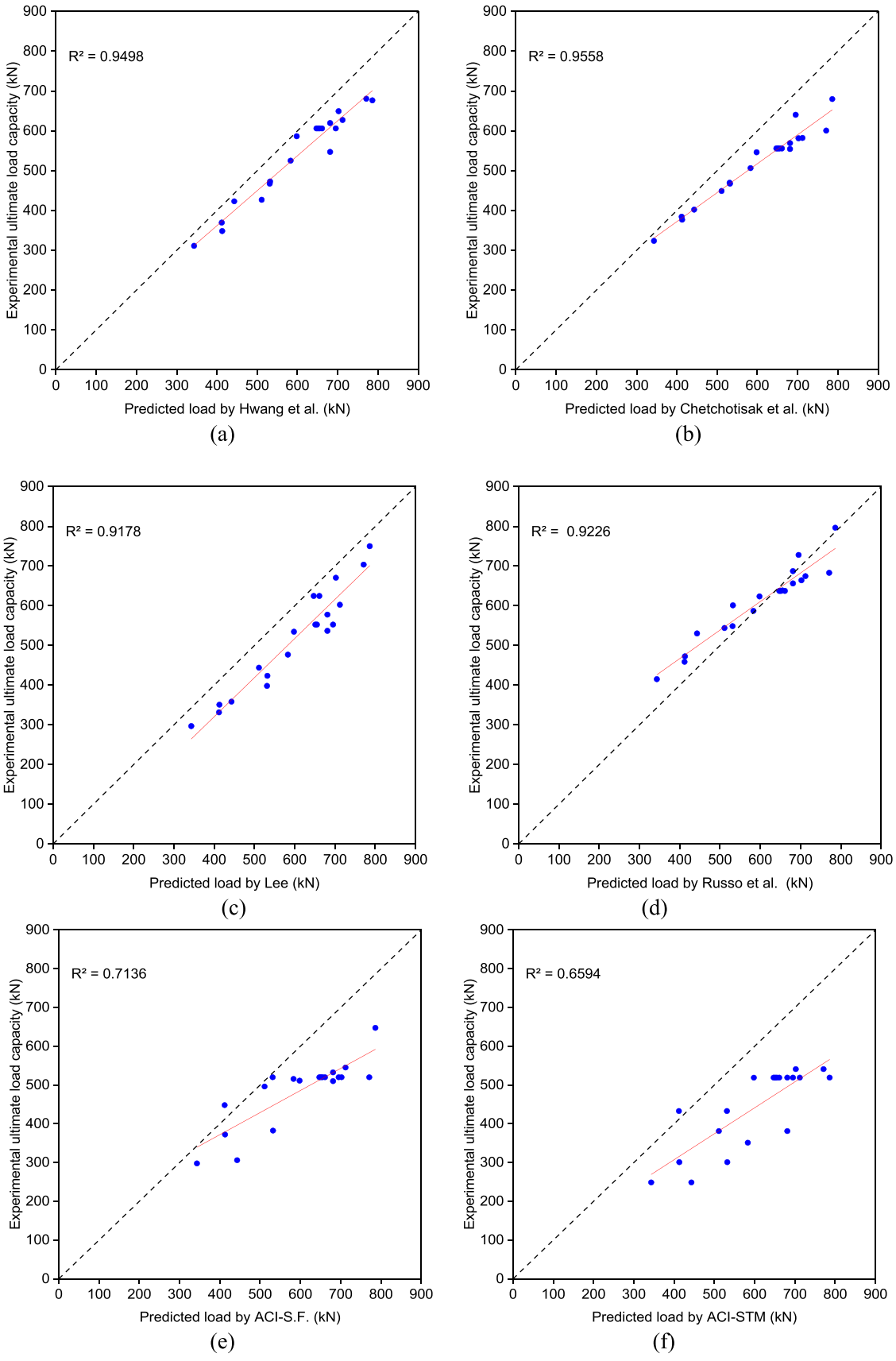

Fig. 11. Comparison of experimental results with theoretically calculated values.

coefficient of variations (COVs) of 4.8 and 5.1 %, respectively. This is further depicted in the Table 12 and the Figs. 11(a) and 11(b).

Furthermore, the models employed by (MSSTM) developed by Lee et al. (2023) and the model proposed by Russo 2006 yielded satisfactory results, with COV of 7.3 and 8.1 %, respectively, as shown in Figs. 11(c) and 11(d). In contrast, the results obtained from the American code ACI 318 [54]) utilizing SF and STM methods provided conservative estimates with COVs of 11.8 and 15.8 %, respectively, as shown in Figs. 11 (e) and 11(f). Notably, the SF method produced more accurate results than the STM method because the SF method is more common for models with $a/d \geq 1$ [97].

As previously demonstrated, increasing the replacement ratio of recycled aggregate had a minimal impact on compressive strength. The mathematical equations mentioned incorporated compressive strength as a significant factor in their derivation, given that recycled aggregate has a negligible influence on compressive strength. Consequently, these equations can be utilized to estimate the (ULC) of concrete corbels made from recycled concrete. The values obtained using the mathematical equations suggested in the literature were found to be very close to the experimental results.

It is clear from the above that the method proposed by Hwang et al. (2017) demonstrated greater accuracy compared to other approaches due to its distinct representation of the disturbed (D-region), which addresses shear strength in discontinuity region failing under diagonal compression. It accounted for material properties and boundary conditions consistent with experimental models. The model, based on a softened strut-and tie framework, simplified computational by analyzing the effects of key variables on the strength of d-region members. Termed the "geometric approximation model" it aligns well with the softened strut-and-tie model while offering comparable accuracy with significantly reduced computational effort. Validation through 449 tests of various structural elements such as deep beams, corbels, squat walls, and beam-column joints confirm its reliability and efficiency.

Theoretical equations that align well with experimental results play a fundamental role in developing global design code equations by providing reliable and robust models for practical applications. Their accuracy ensures consistency and resilience, enabling wide applicability across diverse scenarios. By bridging theoretical predictions with real-world conditions through experimental validation, these equations became strong candidates for adoption in global design codes. Furthermore, their integration enhances predictive accuracy, reduces error, and minimizes on costly and time-intensive experimental testing.

5. Summary and conclusion

In this study, the behavior of reinforced concrete corbels made with recycled coarse aggregate was experimentally investigated. Twenty specimens were constructed and examined, divided into five Groups depending on the variable type.

The ultimate load capacity, load-deflection curves, crack pattern, initial stiffness, and energy dissipation capacity were investigated. The experimental load capacity was compared with ACI provisions and previous literature. The important results obtained are as follows:

1. Increasing The RCA replacement ratio reduced compressive strength by 5.2 %,10.4 %, and 14.0 % for replacement ratios of 20 %,40 %, and 60 %, respectively, and slightly decreased splitting tensile strength. However, the slump remained unaffected due to the SSD conditions of aggregate.
2. The ultimate load capacity of corbels decreased with higher RCA replacement ratios (reductions of 4.4 %, 8.6 %, and 16 % for 20 %,40 %, and 60 %, respectively) but improved significantly with increase with increases in secondary and maim reinforcement steel ratios.
3. High RCA replacement ratios and large shear span-effective depth ratios increase the load-deflection response, while increased secondary and main reinforcement ratios reduced it. Hight-compressive strength specimens exhibited less pronounced load-deflection responses.
4. Crack patterns and failure modes in RCA corbels resembled those of natural aggregate corbels. Initial stiffness slightly decreased with higher RCA replacement ratios but improved with increased reinforcement ratios. Energy dissipation capabilities showed minimal change with varying RCA ratios.
5. Predicting the ultimate load capacity using the SSTM model developed by Hwang et al. (2017) and the MISTM method proposed by Chetchotisak et al. (2022) exhibited the closest alignment with experimental results. In contrast, the results derived from the ACI code were more conservative.

The present study focuses on examining the impact of recycled concrete aggregate (RCA) on various properties of RC corbels. Future research should expand this exploration to include the effects of higher replacement ratios, long-term durability, and performance under dynamic loading conditions. Investigating these aspects will provide a deeper understanding of RCA behavior and enhance confidence in its application in concrete structures.

CRediT authorship contribution statement

Kadhim Z. Naser: Writing – original draft, Methodology, Data curation, Conceptualization. **Abdulamir Atalla Almayah:** Software, Project administration, Investigation, Formal analysis. **Abdulnasser M. Abbas:** Writing – review & editing, Validation, Methodology.

Declaration of competing interest

The authors declare that they have no known competing financial interests or personal relationships that could have appeared to influence the work reported in this paper.

Data availability

Data will be made available on request.

References

[1] Y.C. Hao Yuan, Lintao Kang, Tianyang Geng, Kaize Ma, Compressive axial load performance of GFRP–Confined recycled aggregate concrete–Filled steel tube stub columns, J. Constr. Steel Res. 220 (2024) 108835, https://doi.org/10.1016/j.jcsr.2024.108835.
[2] L.W. Jiongfeng Liang, Wanjie Zou, Wei Li, Compressive behavior of partially encased recycled aggregate concrete columns after exposure to elevated temperature, J. Constr. Steel Res. 221 (2024) 108889, https://doi.org/10.1016/j.jcsr.2024.108889.
[3] C.L. Dongming Huang, Zhenzhen Liu, Yiyan Lu, Shan Li, Compressive behaviors of steel Fiber-reinforced geopolymer recycled aggregate concrete-filled GFRP tube columns, Structures 66 (2024) 106829, https://doi.org/10.1016/j.istruc.2024.106829.
[4] Thanongsak Imjai, Pakjira Aosai, Reyes Garcia, Sudharshan N. Raman, Sandeep Chaudhary, Deflections of high-content recycled aggregate concrete beams reinforced with GFRP bars and steel fibres, Eng. Struct. 312 (2024) 118247, https://doi.org/10.1016/j.engstruct.2024.118247.
[5] Shuo Feng, Ying Jiang, Jingjing Lyu, Huigang Xiao, Qingsong Zhang, Runzhao Song, Junjie Zhang, Zunchao Ren, Effect of nanosilica and Fiber on mechanical properties and microstructure of recycled coarse aggregates road concrete, Constr. Build. Mater. 428 (2024) 136404, https://doi.org/10.1016/j.conbuildmat.2024.136404.
[6] Maurício P. Ferreira, Iana I.R. Damasceno, Manoel J.M.Pereira Filho, Aarão F. Lima Neto, Marcos H. Oliveira, A Jayron, Ribeiro Júnior, Effect of recycled concrete aggregates on the punching strength of slab-column connections without shear reinforcement, J. Build. Eng. 95 (2024) 110174, https://doi.org/10.1016/j.jobe.2024.110174.
[7] Dinesh Kumar, Kanta Rao, Lakshmy Parameshwaran, Engineering and microstructural properties of self-compacting concrete containing coarse recycled concrete aggregate, Mag. Concr. Res. (2024), https://doi.org/10.1680/jmacr.23.00338.
[8] Xiangqian Ye, Yuanyuan Chen, Hailu Yang, Yanmao Xiang, Zhoujing Ye, Wenyu Li, Chichun Hu, Enhancing self-healing of asphalt mixtures containing recycled concrete aggregates and reclaimed asphalt pavement using induction

heating, Constr. Build. Mater. 439 (2024) 137361, https://doi.org/10.1016/j.conbuildmat.2024.137361.
[9] Xutao Zhang, Junyu Wang, Chao Lou, Experimental study on axial tensile properties of basalt fibre reinforced recycled aggregate concrete, Heliyon. 10 (2024) e34208, https://doi.org/10.1016/j.heliyon.2024.e34208.
[10] Zhi-Wei Yan, Yu-Lei Bai, Qiang Zhang, Jun-Jie Zeng, Experimental study on dynamic properties of flax Fiber reinforced recycled aggregate concrete, J. Build. Eng. 80 (2023) 108135, https://doi.org/10.1016/j.jobe.2023.108135.
[11] Changqing Wang, Jian Guo, Liyuan Cao, Youchao Zhang, Chunxiang Li, Zhiming Ma, Mechanical behavior and Fiber reinforcing mechanism of high-toughness recycled aggregate concrete under high strain-rate impact loads, Available online, Constr. Build. Mater. 437 (26 July 2024) 136960.
[12] Shahzadi Irum, Faisal Shabbir, Performance of fly ash/GGBFS based geopolymer concrete with recycled fine and coarse aggregates at hot and ambient curing, J. Build. Eng. 95 (2024) 110148, https://doi.org/10.1016/j.jobe.2024.110148.
[13] Yingjie Xu, Hongniao Chen, Yihui Liang, Jie Shen, Huaxiang Yang Study on fracture characteristics and fracture mechanism of fully recycled aggregate concrete using AE and DIC techniques - ScienceDirect available online: https://www.sciencedirect.com/science/article/abs/pii/S0950061824006810.
[14] M. Alamri, T. Ali, H. Ahmed, M.Z. Qureshi, A. Elmagarhe, M. Adil Khan, A. Ajwad, M. Sarmad Mahmood, Enhancing the engineering characteristics of sustainable recycled aggregate concrete using fly ash, metakaolin and silica fume, Heliyon. 10 (2024) e29014, https://doi.org/10.1016/j.heliyon.2024.e29014.
[15] A. Al-Hussein, F.H. Majeed, K.Z. Naser, Tension lap splices in recycled-aggregate concrete strengthened with steel–Polyolefin fibers, Fibers 12 (2024) 60, https://doi.org/10.3390/fib12080060.
[16] H.-M. Li, J.-Y. Zheng, S.-S. Li, Shear bearing capacity prediction of steel-Fiber-reinforced high-strength concrete corbels on modified compression field theory, Buildings 14 (2024) 388, https://doi.org/10.3390/buildings14020388.
[17] S.-S. Li, J.-Y. Zheng, F.-J. Zhang, H.-M. Li, M.-X. Jia, Z.-J. Liu, A.-J. Chen, W. Xie, Prediction of shear strength for steel-Fiber high-strength concrete corbels with the softened strut-and-tie model, Buildings 13 (2023) 1107, https://doi.org/10.3390/buildings13041107.
[18] S.-S. Li, J.-Y. Zheng, J.-H. Zhang, H.-M. Li, G.-Q. Guo, A.-J. Chen, W. Xie, Experimental investigation on shear capacity of steel-Fiber-reinforced high-strength concrete corbels, Materials. (Basel) 16 (2023) 3055, https://doi.org/10.3390/ma16083055.
[19] Y.M. Neuberger, M.V. Andrade, A.M.D. De Sousa, M. Bandieira, E.P. Da Silva Júnior, H.F. Dos Santos, B. Catoia, E.A. Bolandim, V.B. De Moura Aquino, A. L. Christoforo, et al., Numerical analysis of reinforced concrete corbels using concrete damage plasticity: ssensitivity to material parameters and comparison with analytical models, Buildings 13 (2023) 2781, https://doi.org/10.3390/buildings13112781.
[20] Ygor Moriel Neuberger, Daniel de Lima Araújo, An improved analytical model for two-step corbels in a precast concrete system, Eng. Struct. 284 (2023) 115947, https://doi.org/10.1016/j.engstruct.2023.115947.
[21] Adam Svoboda, Ladislav Klusáček, Lukáš Bobek, Effective strengthening of reinforced concrete corbels using post-tensioning, Eng. Struct. 305 (2024) 117716, https://doi.org/10.1016/j.engstruct.2024.117716.
[22] Patomphop Wongtala, Nida Chaimoon, Nantawat Khomwan, Krit Chaimoon, Experimental and numerical study on structural behavior of reactive powder concrete corbels without stirrups, Case stud. Constr. Mater. 19 (2023) e02372, https://doi.org/10.1016/j.cscm.2023.e02372.
[23] Ankit Borgohain, Ahmed G. Bediwy, F.El-Salakawy Ehab, Practical evaluation of high-strength concrete corbels reinforced with GFRP bent bars, Eng. Struct. 299 (2024) 117095, https://doi.org/10.1016/j.engstruct.2023.117095.
[24] A. Kheyroddin, S. Raygan, M. Kioumarsi, Strut and tie model for CFRP strengthened reinforced concrete corbels, Eng. Struct. 304 (2024) 117609, https://doi.org/10.1016/j.engstruct.2024.117609.
[25] A.H. Chkheiwer, M.A. Ahmed, K.Z. Naser, Modified prediction approach of strength of high strength polyolefin Fiber reinforced concrete corbels, Period. Eng. Nat. Sci. PEN 9 (2021), https://doi.org/10.21533/pen.v9i2.2285.
[26] Giuseppe Campione, Performance of steel fibrous reinforced concrete corbels subjected to vertical and horizontal loads, J. Struct. Eng. 135 (5) (2009). ASCE.
[27] Giuseppe Campione, Flexural response of FRC Corbels, Cem. Concr. Compos. 31 (2009) 204–210. Vol.
[28] Ayad A. Abdul-Razzak, Ahmed A.Mohammed Ali, Modelling and numerical simulation of high strength Fiber reinforced concrete corbels, Appl. Math Model 35 (2011) 2901–2915. Elsevier.
[29] Ayad A. Abdul-Razzak, Ahmed A.Mohammed Ali, Influence of cracked concrete models on the nonlinear analysis of high strength steel fibre reinforced concrete corbels, Compos. Struct. 93 (2011) 2277–2287, 2011.
[30] Atif M.Abdel Hafez, Mohamed M. Ahmed, Hesham Diab, Ahmed Attia M. Drar, Shear behaviour of high strength Fiber reinforced concrete corbels, J. Eng. Sci., Assiut University 40 (4) (2012) 969–987.
[31] Mohammed M. Salman, Ihsan Al-Shaarbaf, Jassim M. Aliewi, Experimental study on the behavior of normal and high strength self-compacting reinforced concrete corbels, J. Eng. Dev. 18 (6) (2014). ISSN 1813- 7822.
[32] I. Ivanova, J. Assih, A. Li, D. Dontchev, Y. Delmas, Experimental investigation into strengthened short reinforced concrete corbels by bonding carbon Fiber fabrics, J. Adhes. Sci. Technol. 29 (2015) 2176–2189, https://doi.org/10.1080/01694243.2015.1060060.
[33] J. Assih, I. Ivanova, D. Dontchev, A. Li, Concrete damaged analysis in strengthened corbel by external bonded carbon fibre fabrics, Appl. Adhes. Sci. 3 (2015) 21, https://doi.org/10.1186/s40563-015-0045-1.
[34] E. K. Sayhood, Q. Abdul Majeed Hassan, L. A. Gh. Yassin, Enhancement in the load-carrying capacity of reinforced concrete corbels strengthened with CFRP strips under monotonic or repeated loads, Eng. Technol. J. 34 (2016) 2705–2719, https://doi.org/10.30684/etj.34.14A.14.
[35] Layla A. Yassin, Ph.D. A Thesis, University of Baghdad, 2016.
[36] I. Ivanova, J. Assih, The effect of fatigue test on short reinforced-concrete corbel strengthened by externally bonded composite fibre fabrics, Eng. Fract. Mech. 167 (2016) 167–175, https://doi.org/10.1016/j.engfracmech.2016.04.035.
[37] Y. Al-Kamaki, G. Hassan, G. Alsofi, Experimental study of the behaviour of RC corbels strengthened with CFRP sheets. *Case stud*, Constr. Mater. 9 (2018), https://doi.org/10.1016/j.cscm.2018.e00181.
[38] K. Satish, S. Kumar, B. Rai, Fly ash induced self compacting concrete with recycled concrete aggregate, Int. J. Mech. Solids 12 (2017) 151–168. *ISSN 0973-1881*.
[39] E.A. Sulaiman, Jamal A. Khudair, Experimental study on the behavior and strength of reinforced concrete corbels cast with self-compacting concrete incorporating recycled concrete AS coarse aggregate, IJCIET 10 (1) (2019) 188–201.
[40] A. Emadaldeen, E.A.S. Sulaiman, J. Khudair, Effect of using recycled concrete aggregate on behavior of r.C corbels cast with self-compacting concrete (experimental and analytical study), Kufa J. Eng. 11 (2020) 1–21, https://doi.org/10.30572/2018/KJE/110101.
[41] A.Z. Hamoodi, A.H. Chkheiwer, J.A. Kadim, Shear strength of reinforced recycled aggregate concrete corbels, J. Eng. 2021 (2021) 1–10, https://doi.org/10.1155/2021/6652647.
[42] Q.M. Shakir, Response of innovative high strength reinforced concrete encased-composite corbels, Structures 25 (2020) 798–809, https://doi.org/10.1016/j.istruc.2020.03.056.
[43] ASTM International, ASTM C 150/C150M-19, Standard Specification For Portland Cement, ASTM International, Pennsylvania, United States, 2019, https://doi.org/10.1520/C0150_C0150M-22.
[44] ASTM C33/C33M-23, Standard Specification for Concrete Aggregates, International, Pennsylvania, United States, 2023.
[45] ASTM C29/C29M-23, Standard test method for bulk density (“Unit Weight”) and voids in aggregate available online: https://www.astm.org/c0029_c0029m-23.html.
[46] ASTM C127-15,Standard test method for relative density (Specific Gravity) and absorption of coarse aggregate available online: https://www.astm.org/c0127-15.html.
[47] ASTM C494/C494M-19,Standard Specification for Chemical Admixtures For Concrete . ASTM International, West Conshohocken Available online: https://www.astm.org/c0494_c0494m-19e01.html.
[48] ASTM A615/A615M-24, Standard specification for deformed and plain carbon-steel bars for concrete reinforcement available online: https://www.astm.org/a0615_a0615m-24.html.
[49] ACI Committee 211. Standard practice for selecting proportions for normal, heavyweight, and mass concrete. Farmington Hills, MI, USA: farmington Hills; 1991. Available online: https://www.concrete.org/store/productdetail.aspx?ItemID=211122&Language=English&Units=US_Units.
[50] ASTM C143/C143M-20 Standard test method for slump of hydraulic cement concrete available online: https://www.astm.org/astm-tpt-168.html.
[51] ASTM C39/C39M-21, Standard test method for compressive strength of cylindrical concrete specimens. Available online: https://www.astm.org/c0039_c0039m-21.html.
[52] BS EN 12390-3,(2019). Testing hardened concrete. Compressive strength of test specimens.
[53] ASTM C496/C496M-17, Standard test method for splitting tensile strength of cylindrical concrete specimens available online: https://www.astm.org/c0496_c0496m-17.html.
[54] ACI 318-19, Building Code Requirements For Structural Concrete and Commentary, American Concrete Institute, 2019. ISBN 978-1-64195-056-5.
[55] N.A. Jokhio, B.A. Memon, S.A. Malah, M. Oad, M.A. Memon, R.A. Bhanbhro, Workability and strength of recycled aggregate concrete reinforced with nylon fibers, Mehran Univ. Res. J. Eng. Technol. 43 (2024) 34, https://doi.org/10.22581/muet1982.2850.
[56] B. Nachimuthu, R. Viswanathan, Y. Subramaniyan, J. Baskaran, Mechanical properties of recycled concrete aggregates with superplasticizer, Matér. Rio 29 (2024) e20230382, https://doi.org/10.1590/1517-7076-rmat-2023-0382. *Jan.*.
[57] W. Alnahhal, Flexural behavior of basalt Fiber reinforced concrete beams with recycled concrete coarse aggregates, Constr. Build. Mater. (2018).
[58] A. Abushanab, W. Alnahhal, Flexural behavior of reinforced concrete beams prepared with treated wastewater, recycled concrete aggregates, and fly ash, Structures 45 (2022) 2067–2079, https://doi.org/10.1016/j.istruc.2022.10.029.
[59] R. Hameed, M. Tahir, S. Abbas, H.U. Sheikh, S.M.S. Kazmi, M.J. Munir, Mechanical and durability characterization of hybrid recycled aggregate concrete, Materials. (Basel) 17 (2024) 1571, https://doi.org/10.3390/ma17071571.
[60] Q. Mohammed Shakir, A.F. Alghazali, New model of eco-friendly hybrid deep beams with wastes of crushed concrete, J. Teknol. 85 (2023) 145–154, https://doi.org/10.11113/jurnalteknologi.v85.20431.
[61] Q. Ma, J. Xiao, T. Ding, Z. Duan, M. Song, X. Cao, The prediction of compressive strength for recycled coarse aggregate concrete in cold region. *Case stud*, Constr. Mater. 19 (2023) e02546, https://doi.org/10.1016/j.cscm.2023.e02546.
[62] T. Imjai, P. Aosai, R. Garcia, S.N. Raman, S. Chaudhary, Deflections of high-content recycled aggregate concrete beams reinforced with GFRP bars and steel

fibres, Eng. Struct. 312 (2024) 118247, https://doi.org/10.1016/j.engstruct.2024.118247.
[63] M. Alharthai, T. Ali, M.Z. Qureshi, H. Ahmed, The enhancement of engineering characteristics in recycled aggregates concrete combined effect of fly ash, silica fume and PP Fiber, Alex. Eng. J. 95 (2024) 363–375, https://doi.org/10.1016/j.aej.2024.03.084.
[64] Y. Liang, Fracture behaviors of sustainable recycled aggregate concrete under compression-shear loading: llaboratory test, numerical simulation, and environmental safety analysis, Case Stud. Constr. Mater. 20 (2024) e03328, https://doi.org/10.1016/j.cscm.2024.e03328.
[65] L. Marku, K. Beleshi, E. Zhabjaku, A review of coarse recycled aggregate in concrete applications, Am. J. Eng. Res. (2024).
[66] N.A. Abdulla, Role of coarse recycled aggregate in concrete beams, Mater. 4 (2024) 100216, https://doi.org/10.1016/j.nxmate.2024.100216.
[67] D. Trento, F. Faleschini, V. Revilla-Cuesta, V. Ortega-López, Improving the early-age behavior of concrete containing coarse recycled aggregate with raw-crushed wind-turbine blade, J. Build. Eng. 92 (2024) 109815, https://doi.org/10.1016/j.jobe.2024.109815.
[68] A. Zarei, M. Sharghi, H. Jeong, H. Afshin, A comparative evaluation of modification methods for improving the mechanical properties of recycled aggregate-recycled steel Fiber concrete, KSCE J. Civ. Eng. (2024), https://doi.org/10.1007/s12205-024-0005-z.
[69] O.A. Qasim, N. Hilal, M.I. Al Biajawi, N.H. Sor, T.A. Tawfik, Studying the usability of recycled aggregate to produce new concrete, J. Eng. Appl. Sci. 71 (2024) 129, https://doi.org/10.1186/s44147-024-00463-1.
[70] C. Lu, Q. Yu, J. Wei, Y. Niu, Y. Zhang, C. Lin, P. Yang, Influence of interface transition zones (ITZ) and pore structure on the compressive strength of recycled aggregate concrete, Constr. Build. Mater. 456 (2024) 139299.
[71] Y. Li, T. Fu, R. Wang, Y. Li, An assessment of microcracks in the interfacial transition zone of recycled concrete aggregates cured by CO2, Constr. Build. Mater. 236 (2020) 117543.
[72] X.S. Shi, F.G. Collins, X.L. Zhao, Q.Y. Wang, Mechanical properties and microstructure analysis of fly ash geopolymeric recycled concrete, J. Hazard. Mater. 237 (2012) 20–29.
[73] F. Al Mahmoud, R. Boissiere, C. Mercier, A. Khelil, Shear behavior of reinforced concrete beams made from recycled coarse and fine aggregates, Structures 25 (2020) 660–669, https://doi.org/10.1016/j.istruc.2020.03.015.
[74] M. Elsayed, S.R. Abd-Allah, M. Said, A.A. El-Azim, Structural performance of recycled coarse aggregate concrete beams containing waste glass powder and waste aluminum fibers. *Case stud*, Constr. Mater. 18 (2023) e01751, https://doi.org/10.1016/j.cscm.2022.e01751.
[75] K.N. Rahal, K. Elsayed, Shear strength of 50 MPa longitudinally reinforced concrete beams made with coarse aggregates from low strength recycled waste concrete, Constr. Build. Mater. 286 (2021) 122835, https://doi.org/10.1016/j.conbuildmat.2021.122835.
[76] I.S. Ignjatović, S.B. Marinković, N. Tošić, Shear behaviour of recycled aggregate concrete beams with and without Shear reinforcement, Eng. Struct. 141 (2017) 386–401, https://doi.org/10.1016/j.engstruct.2017.03.026.
[77] D. Gao, W. Zhu, D. Fang, J. Tang, H. Zhu, Shear behavior analysis and capacity prediction for the steel Fiber reinforced concrete beam with recycled fine aggregate and recycled coarse aggregate, Structures 37 (2022) 44–55, https://doi.org/10.1016/j.istruc.2021.12.075.
[78] S. Seara-Paz, B. González-Fonteboa, F. Martínez-Abella, J. Eiras-López, Deformation recovery of reinforced concrete beams made with recycled coarse aggregates, Eng. Struct. 251 (2022) 113482, https://doi.org/10.1016/j.engstruct.2021.113482.
[79] C. Lu, Q. Yu, J. Wei, Y. Niu, Y. Zhang, C. Lin, P. Yang, Influence of interface transition zones (ITZ) and pore structure on the compressive strength of recycled aggregate concrete, Constr. Build. Mater. 456 (2024) 139299.
[80] Song GAO, et al., Study on the influence of the properties of interfacial transition zones on the performance of recycled aggregate concrete, Constr. Build. Mater. 408 (2023) 133592.
[81] A. Djerbi, Effect of recycled coarse aggregate on the new interfacial transition zone concrete, Constr. Build. Mater. 190 (2018) 1023–1033.
[82] A. Vahidi, A. Mostaani, A.T. Gebremariam, F. Di Maio, P. Rem, Feasibility of utilizing recycled coarse aggregates in commercial concrete production, J. Clean. Prod. 474 (2024) 143578.
[83] V.W. Tam, H. Wattage, K.N. Le, A. Buteraa, M. Soomro, Methods to improve microstructural properties of recycled concrete aggregate: a critical review, Constr. Build. Mater. 270 (2021) 121490.
[84] Y. Zhao, W. Zeng, H. Zhang, Properties of recycled aggregate concrete with different water control methods, Constr. Build. Mater. 152 (2017) 539–546.
[85] C. Liang, H. Chen, R. Li, W. Chi, S. Wang, S. Hou, P. Zhang, Effect of additional water content and adding methods on the performance of recycled aggregate concrete, Constr. Build. Mater. 423 (2024) 135868.
[86] Z. Li, J. Liu, J. Xiao, P. Zhong, A method to determine water absorption of recycled fine aggregate in paste for design and quality control of fresh mortar, Constr. Build. Mater. 197 (2019) 30–41.
[87] M.John Robert Prince, Bhupinder Singh, Bond behaviour of deformed steel bars embedded in recycled aggregate concrete, Constr. Build. Mater. 49 (2013) 852–862.
[88] K. Pandurangan, A. Dayanithy, S.Om Prakash, Influence of treatment methods on the bond strength of recycled aggregate concrete, Constr. Build. Mater. 120 (2016) 212–221.
[89] Jianzhuang Xiao, H.Bond Falkner, Behaviour between recycled aggregate concrete and steel rebars, Constr. Build. Mater. 21 (2) (2007) 395–401.
[90] W.H. Kwan, M. Ramli, K.J. Kam, M.Z. Sulieman, Influence of the amount of recycled coarse aggregate in concrete design and durability properties, Constr. Build. Mater. 26 (1) (2012) 565–573.
[91] Sami W. Tabsh, Akmal S Abdelfatah, Influence of recycled concrete aggregates on strength properties of concrete, Constr. Build. Mater. 23 (2) (2009) 1163–1167.
[92] K.S. Abdul-Razzaq, A.A. Dawood, Corbel Strut and tie modeling – Experimental verification, Structures 26 (2020) 327–339, https://doi.org/10.1016/j.istruc.2020.04.021.
[93] S.Kh. Faleh, A.H. Chkheiwer, I.S Saleh, Structural behavior of high-strength concrete corbels involving steel fibers or closed stirrups, Period. Eng. Nat. Sci. PEN 10 (2022) 239, https://doi.org/10.21533/pen.v10i1.2604.
[94] I.S. Saleh, S.Kh. Faleh, M.Sh Mahdi, Effects of Fiber type and shape on the shear behavior of reinforced concrete corbels without hoop re-bars, Civ. Eng. J. 8 (2022) 519–530, https://doi.org/10.28991/CEJ-2022-08-03-08.
[95] F. J., A.-T.; A. M., A., Structural behavior of reinforced concrete corbel using high-strength materials under monotonic and repeated loads, Int. J. Appl. Sci. 2 (2019) 1, https://doi.org/10.30560/ijas.v2n2p1.
[96] Rezaei, M.; Osman, S.A.; Shanmugam, N.E. Primary and secondary reinforcements in Corbels under combined action of vertical and horizontal loadings.
[97] Khattab Saleem Abdul-Razzaq, Reinforcing struts and ties in concrete corbels, ACI Struct. J. 118 (2021), https://doi.org/10.14359/51732650.
[98] K.N. Rahal, Y.T. Alrefaei, Shear strength of recycled aggregate concrete beams containing stirrups, Constr. Build. Mater. 191 (2018) 866–876, https://doi.org/10.1016/j.conbuildmat.2018.10.023.
[99] A. Lapko, R. Grygo, Studies of RC beams made of recycling aggregate concrete strengthened with the HSC-HPC inclusions, Procedia Eng. 57 (2013) 678–686, https://doi.org/10.1016/j.proeng.2013.04.086.
[100] S. Ahmed, A. El-Zohairy, A. Eisa, M. Mohamed, A. Abdo, Experimental investigation of self-compacting concrete with recycled concrete aggregate, Buildings 13 (2023) 856, https://doi.org/10.3390/buildings13040856.
[101] S. Arabiyat, M. Abdel Jaber, H. Katkhuda, N. Shatarat, Influence of using two types of recycled aggregates on shear behavior of concrete beams, Constr. Build. Mater. 279 (2021) 122475, https://doi.org/10.1016/j.conbuildmat.2021.122475.
[102] R. Soltanabadi, K. Behfarnia, Shear strength of reinforced concrete deep beams containing recycled concrete aggregate and recycled asphalt pavement, Constr. Build. Mater. 314 (2022) 125597, https://doi.org/10.1016/j.conbuildmat.2021.125597.
[103] Mahir M. HASON, Mohamed H. MUSSA, Ahmed M ABDULHADI, Flexural ductility performance of hybrid-recycled aggregate reinforced concrete T-beam, Mater. Today: Proc. 46 (2021) 682–688.
[104] M.F. Ojaimi, M.Y. Alabdulhady, K.Z. Naser, Influence of concrete compressive strength on CFRP strengthening and repairing of RC two-way slabs, J. Eng. 2024 (2024) 2166919, https://doi.org/10.1155/2024/2166919.
[105] Ö. Mercimek, R. Ghoroubi, A. Özdemir, Ö. Anil, Y. Erbaş, Investigation of strengthened low slenderness RC column by using textile reinforced mortar strip under axial load, Eng. Struct. 259 (2022) 114191, https://doi.org/10.1016/j.engstruct.2022.114191.
[106] A. Türer, Ö. Mercimek, Ö. Anıl, Y. Erbaş, Experimental and numerical investigation of punching behavior of two-way RC slab with different opening locations and sizes strengthened with CFRP strip, Structures 49 (2023) 918–942, https://doi.org/10.1016/j.istruc.2023.01.157.
[107] K. Rahal, Mechanical properties of concrete with recycled coarse aggregate, Build. Environ. 42 (1) (2007) 407–415.
[108] S.W. Tabsh, A.S. Abdelfatah, Influence of recycled concrete aggregates on strength properties of concrete, Constr. Build. Mater. 23 (2) (2009) 1163–1167.
[109] H. Zhao, A. Zhou, L. Zhang, A. Arulrajah, A novel three-dimensional DEM model for recycled aggregate concrete considering material heterogeneity and microcrack evolution, Compos. Struct. 352 (2025) 118677.
[110] Hwang Shear, Strength prediction for reinforced concrete corbels, ACI Struct. J. 97 (2000), https://doi.org/10.14359/7419.
[111] S.-J. Hwang, R.-J. Tsai, W.-K. Lam, J.P. Moehle, Simplification of softened strut-and-tie model for strength prediction of discontinuity regions, ACI Struct. J. 114 (2017), https://doi.org/10.14359/51689787.
[112] Russo reinforced concrete corbels - shear strength model and design formula, ACI Struct. J. 103 (2006), https://doi.org/10.14359/15080.
[113] P. Chetchotisak, J. Teerawong, S. Yindeesuk, Modified interactive strut-and-tie modeling of reinforced concrete deep beams and corbels, Structures 45 (2022) 284–298, https://doi.org/10.1016/j.istruc.2022.08.116.
[114] S.-S. Li, D. Peng, H. Wang, F.-J. Zhang, H.-M. Li, Y.-J. Xie, A.-J. Chen, W. Xie, Analysis of shear model for steel-Fiber-reinforced high-strength concrete corbels with welded-Anchorage longitudinal reinforcement, Mater. (Basel) 16 (2023) 4907, https://doi.org/10.3390/ma16144907.